Biochemical and Biophysical Research Communications 379 (2009) 38–42

Contents lists available at ScienceDirect

Biochemical and Biophysical Research Communications

journal homepage: www.elsevier.com/locate/ybbrc

Characterization of diabetic nephropathy in CaM kinase IIα (Thr286Asp) transgenic mice

Hikari Suzuki [a], Ichiro Kato [b,*], Isao Usui [a], Ichiro Takasaki [c], Yoshiaki Tabuchi [c], Takeshi Oya [d], Koichi Tsuneyama [e], Hiroshi Kawaguchi [b], Koichi Hiraga [b], Shin Takasawa [f,g], Hiroshi Okamoto [g], Kazuyuki Tobe [a], Masakiyo Sasahara [d]

[a] First Department of Internal Medicine, University of Toyama Graduate School of Medicine and Pharmaceutical Sciences, Toyama 930-0194, Japan
[b] Department of Biochemistry, University of Toyama Graduate School of Medicine and Pharmaceutical Sciences, Sugitani 2630, Toyama 930-0194, Japan
[c] Division of Molecular Genetics, Life Scientific Research Center, University of Toyama, Toyama 930-0194, Japan
[d] Department of Pathology, University of Toyama Graduate School of Medicine and Pharmaceutical Sciences, Toyama 930-0194, Japan
[e] Department of Diagnostic Pathology, University of Toyama Graduate School of Medicine and Pharmaceutical Sciences, Toyama 930-0194, Japan
[f] Department of Biochemistry, Nara Medical University, Kashihara 634-8521, Japan
[g] Department of Advanced Biological Sciences for Regeneration (Kotobiken Medical Laboratories), Tohoku University Graduate School of Medicine, Sendai 980-8575, Japan

ARTICLE INFO

Article history:
Received 17 November 2008
Available online 12 December 2008

Keywords:
Ca^{2+}/calmodulin-dependent protein kinase II
Diabetes
Transgenic mice
cDNA microarray
Nephropathy
Macrophage
Osteopontin
Cyclin D2

ABSTRACT

Detailed studies were performed on diabetic kidneys derived from transgenic mice overexpressing the mutant form (Thr286Asp) of Ca^{2+}/calmodulin-dependent protein kinase IIα (CaM kinase IIα) in pancreatic β-cells. Kidney weight/body weight ratio, urinary albumin/creatinine ratio, serum BUN level, and mesangial/glomerular area ratio were all significantly higher in transgenic mice than in wild-type mice. cDNA microarray analysis revealed 17 up-regulated genes and 12 down-regulated genes in transgenic kidney. Among up-regulated genes, cyclin D2 (6.70-fold) and osteopontin (2.35-fold) were thought to play important roles in the progression of diabetic nephropathy. Transgenic glomeruli and tubular epithelial cells were strongly stained for osteopontin, a molecule which induces immune response. In quantitative real-time RT-PCR analyses, expressions of not only M1 macrophage marker genes but also M2 macrophage marker genes were elevated in renal cortex of transgenic mice. Overall results indicate that CaM kinase IIα (Thr286Asp) transgenic mice serve as an excellent model for diabetic nephropathy.

Diabetes mellitus (DM) is the most prevalent and serious metabolic disease in the 21st century. DM is a disease characterized by hyperglycemia and is caused by absolute or relative insulin deficiency, sometimes associated with insulin resistance [1]. As a consequence of its microvascular pathology, DM is the leading cause of blindness, end-stage renal disease, and a variety of neuropathies [2]. Approximately 30% of insulin-dependent DM patients suffered from diabetic nephropathy, eventually underwent renal dialysis or transplantation [3]. Nephropathy is thus a life-threatening complication of DM and is the leading cause of end-stage renal disease in developed countries. The features characteristics of diabetic nephropathy include persistent albuminuria, a progressive decline in renal function, and, histopathologically, mesangial expansion followed by glomerulosclerosis [4]. However, little was known about the molecular mechanisms leading to end-stage renal disease in DM. Spontaneously diabetic animals such as nonobese diabetic (NOD) mice developed only limited lesions such as mild mesangial sclerosis [5]. The same was the case with chemically induced diabetic rodents [6]. To understand the pathogenesis of diabetic nephropathy and to develop preventive and therapeutic methods against it, suitable animal models for this disease were needed.

Recently we generated transgenic (TG) mice overexpressing the mutant form (Thr286Asp) of Ca^{2+}/calmodulin-dependent protein kinase IIα (CaM kinase IIα) in pancreatic β-cells [7]. Western blot and immunohistochemical analyses showed overexpression of CaM kinase IIα in pancreatic β-cells of TG mice. Cell proliferation in TG islets was severely impaired as assessed by in vivo BrdU labeling analysis. NF-κB accumulated in nuclei of TG β-cells at postnatal day (P)21, which were associated with DNA laddering. One hundred percent of TG mice developed severe hypoinsulinemic diabetes by P28. TG mice at P140-P168 developed severe renal and retinal lesions, suggesting that the TG mice will be valuable as a novel model of severe insulin-dependent DM.

In the present study, we performed detailed pathological analyses of the diabetic kidneys in CaM kinase IIα (Thr286Asp) TG

* Corresponding author. Fax: +81 76 434 5014.
E-mail address: ichikato777@yahoo.co.jp (I. Kato).

0006-291X/$ - see front matter © 2008 Elsevier Inc. All rights reserved.
doi:10.1016/j.bbrc.2008.11.143

mice. Furthermore, to identify susceptibility genes for the development of diabetic nephropathy in the TG mice, changes of the gene expression profile in the TG kidneys were surveyed by GeneChip Expression Analysis.

Materials and methods

Diabetic model mice. CaM kinase IIα (Thr286Asp) TG male mice [7] were backcrossed to CD1 female mice (Japan Charles River Inc., Yokohama, Japan) more than five times and males were used in the present study. In all experiments, non-transgenic male littermates were used as controls. CaM kinase IIα (Thr286Asp) TG mice were identified by PCR using primer sets of 5′-CGA AGA TGT GCG ACC CTG GAA TGA C-3′ and 5′-TTT GTC CAA TTA TGT CAC ACC ACA G-3′. The procedures were approved by the Institutional Animal Care and Use Committee guidelines at University of Toyama.

Histology and immunohistochemistry. Mice were deeply anesthetized by an intraperitoneal injection of pentobarbital sodium (1 mg/kg body weight). After the perfusion with ice-cold phosphate buffered saline (PBS) solution, the left kidney was excised, decapsulated, weighed, and immersed in methyl Carnoy's solution. The right kidney was perfused with 4% paraformaldehyde (PFA)/0.1 M phosphate buffer (PB), excised, decapsulated, and immersed in 4% PFA/0.1 M PB. Both kidneys were embedded in paraffin and sections of 4 μm thickness were cut in perpendicular direction to long axis of the kidney for immunohistochemical and morphometric analyses. Sections were routinely stained with hematoxylin and eosin. The tissues fixed in Methyl Carnoy's solution were subjected to an immunohistochemical study using a polyclonal goat antibody against osteopontin (dilution 1:500; sc-10593, Santa Cruz Biotechnology, Santa Cruz, CA). The tissues fixed in 4% PFA/0.1 M PB were subjected to an immunohistochemical study using a polyclonal rat antibody against F4/80 (dilution 1:500; MCAP497, UK-Serotec Ltd., Oxford, UK). For the staining of osteopontin and F4/80, the tissue sections were treated with 3% H_2O_2 containing 0.1% sodium azide for 5 min to block endogenous peroxidase activity. After washing in Tris-buffered saline containing 0.05% Tween 20, the sections were incubated with each primary antibody for overnight at 4 °C. After washing, the sections were incubated for 10 min with Histofine Simple Stain MAX-PO (G) for osteopontin and with Histofine Simple Stain MAX-PO (R) for F4/80 (Nichirei Bioscience, Tokyo, Japan). Diaminobenzidine was used as a chromogen.

Morphometric analysis of the glomeruli. For morphometric analysis of the glomeruli, sections were stained with hematoxylin–eosin. In each animal, 20 glomeruli cut at its vascular pole were subjected for morphometric analyses. A glomerular area was traced along the outline of capillary loop using a computer-assisted color image analyzer VH analyzer (Keyence, Osaka, Japan). Mesangial areas were color-extracted, and calculated by VH analyzer. Percentages of mesangial areas among glomerular areas were calculated.

Phenotypic characterization. The levels of blood glucose and hemoglobin A_{1c} in peripheral blood were determined using Accu-Chek Compact (Roche Diagnostics Corp., Basel, Switzerland) and DCA2000 analyzer (Siemens Healthcare Diagnostics Inc., New York, NY), respectively. Urinary albumin and creatinine levels were determined using ELISA (Albuwell M; Exocell Inc., Philadelphia, PA) and creatinine assay kit (Creatinine Companion; Exocell Inc.), respectively. Blood urea nitrogen (BUN) concentrations were determined using commercial reagent (BUN Kainos; Kainos Laboratory, Tokyo, Japan).

cDNA microarray analysis. Total RNA was extracted from whole kidney at 12 weeks of age using a Trizol reagent (Invitrogen, Carlsbad, CA) and an RNeasy Total RNA Extraction Kit (Qiagen K.K., Tokyo, Japan). Then, RNA samples were treated with RNase-free DNase (Qiagen K.K.) for 15 min at room temperature. cDNA microarray analysis was performed as described [8] using IntelliGene II Mouse CHIP (X2021, Takara Bio Inc., Otsu, Japan), which were spotted with 4285 cDNA fragments of mouse known genes and approximately 300 expressed sequence tags (ESTs). A list of these genes is available at Takara Bio's website (http://www.takara-bio.com/index.htm). Antisense RNA was generated from kidneys by using an RNA transcript SureLABEL Core Kit (Takara Bio Inc.). The antisense RNAs from wild-type (WT) kidney and TG kidney were labeled with Cy3 and Cy5, respectively. Hybridization and washing of the microarray were carried out according to the manufacturer's instructions. The microarrays were scanned in both Cy3 and Cy5 channels with a ScanArray Lite (Packard BioChip Technologies, Billerica, MA). QuantArray software (Packard BioChip Technologies) was used for image analysis. The data were further analyzed using GeneSpringGX software (Agilent Technologies, Santa Clara, CA) to extract the significant genes.

Reverse transcription and quantitative real-time PCR analysis. Total RNA (500 ng) extracted from renal cortex at 20 weeks of age was reverse transcribed using TaqMan Reverse Transcription (RT) Reagents (Applied Biosystems, Foster City, CA). TaqMan real-time quantitative PCR was performed and analyzed according to the manufacturer's instructions. Commercially available primer and probe sets for each gene (Applied Biosystems) were purchased. Ten independent RNA samples were analyzed and normalized to the values for 18S ribosomal RNA, whose level did not show a significant difference between TG mice and WT mice.

Results

Phenotypic characterization of CaM kinase IIα (Thr286Asp) TG mice

The body weight at 20 weeks of age (Fig. 1A) was significantly ($p < 0.001$) less in the TG mice (30.9 ± 1.3 g, $n = 18$) than in the WT mice (44.7 ± 1.5 g, $n = 18$). Blood glucose levels (Fig. 1B) were significantly ($p < 0.001$) higher in the TG mice (792.2 ± 78.8 mg/dl, $n = 13$) than in the WT mice (161.2 ± 12.0 mg/dl, $n = 13$). Hemoglobin A_{1c} levels (Fig. 1C) were also significantly ($p < 0.001$) higher in the TG mice (9.44 ± 0.61%, $n = 8$) than in the WT mice (3.40 ± 0.08%, $n = 13$). The ratios of kidney weight to body weight (Fig. 1D) were significantly ($p < 0.001$) higher in the TG mice (3.76 ± 0.33%, $n = 14$) than in the WT mice (1.37 ± 0.08%, $n = 12$). The ratios of urinary albumin to urinary creatinine (Fig. 1E) were significantly ($p < 0.01$) higher in the TG mice (134.9 ± 27.6 mg/g, $n = 9$) than in the WT mice (17.5 ± 7.4 mg/g, $n = 7$). The BUN levels in the serum (Fig. 1F) were significantly ($p < 0.05$) higher in the TG mice (49.8 ± 6.8 mg/dl, $n = 7$) than in the WT mice (28.6 ± 3.6 mg/dl, $n = 7$).

Histological examination of kidneys

Glomerular injury in the diabetic mice can be characterized by glomerular hyperplasia and mesangial matrix expansion [9]. We examined the histological changes in the WT mice and TG mice at the ages of 4–20 weeks (Fig. 2). The glomerular hyperplasia and mesangial matrix expansion became apparent at 8 weeks of age in the TG mice (Fig. 2G) and continued thereafter (Fig. 2H–J). These lesions were never observed in the WT mice (Fig. 2A–E). Mean glomerular surface area at 20 weeks of age (Fig. 2K) was significantly ($p < 0.001$) larger in the TG mice (9685.1 ± 328.7 μm^2, $n = 60$) than in the WT mice (5371.9 ± 198.1 μm^2, $n = 60$). Mean mesangial area at 20 weeks of age (Fig. 2L) was significantly ($p < 0.001$) larger in the age-matched TG mice (1759.0 ± 148.4 μm^2, $n = 60$) than in the WT mice (513.0 ± 25.8 μm^2, $n = 60$). The ratios of mesangial area to glomerular area (Fig. 2M) were also significantly ($p < 0.001$) higher in the TG mice (17.97 ± 1.00%, $n = 60$) than in the WT mice (10.13 ± 0.35%, $n = 60$).

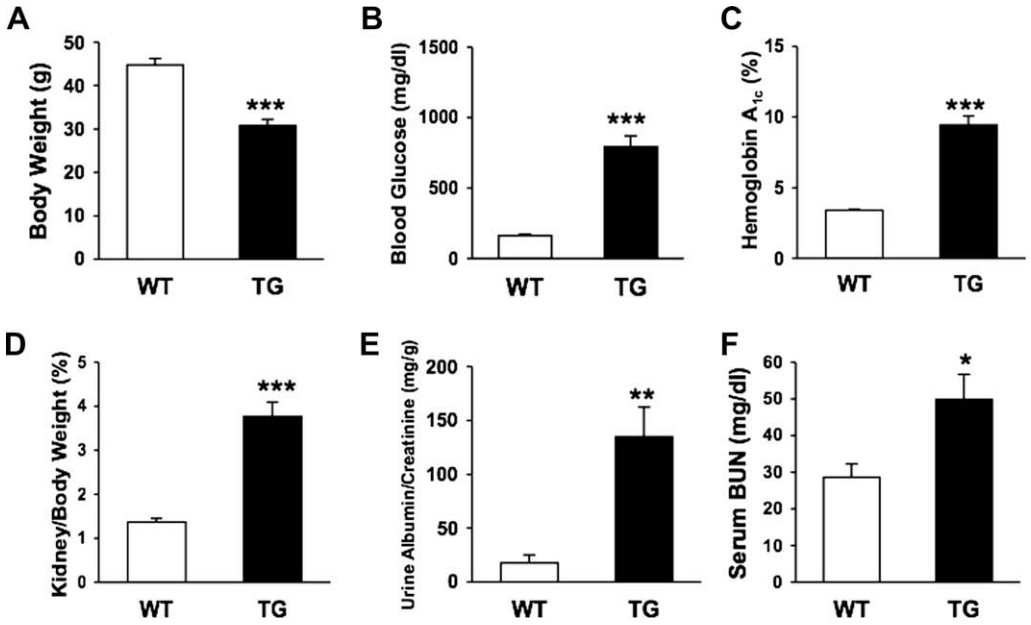

Fig. 1. Phenotypic characterization of WT mice and TG mice at the age of 20 weeks. (A) Body weight. (B) Blood glucose levels. (C) Hemoglobin A_{1c} levels. (D) Kidney weight/body weight ratio. (E) Urine albumin/creatinine ratio. (F) Serum BUN levels. White bars and black bars indicate means ± SE for WT mice and TG mice, respectively. Statistical analyses were performed by Student's *t*-test. $^{*}p < 0.05$; $^{**}p < 0.01$; $^{***}p < 0.001$ compared with the values for age-matched WT mice.

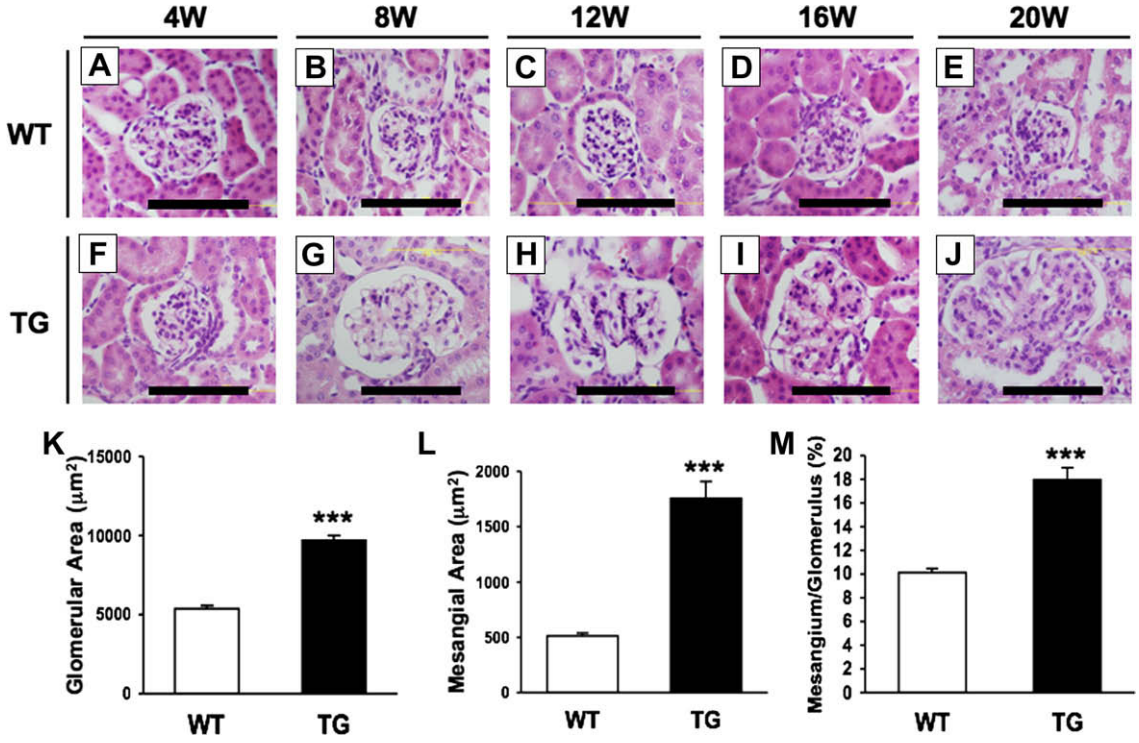

Fig. 2. Hematoxylin–eosin stainings of kidneys from WT mice (A–E) and TG mice (F–J) at the ages of 4 weeks (A, F), 8 weeks (B, G), 12 weeks (C, H), 16 weeks (D, I), and 20 weeks (E, J). Images are representative from studies of $n = 3$ mice for each age. Scale bars = 100 μm. Glomerular area (K), mesangial area (L), and mesangial/glomerular area ratio (M) at 20 weeks of age. White bars and black bars indicate means ± SE for WT mice and TG mice, respectively. Statistical analyses were performed by Student's *t*-test. $^{***}p < 0.001$ compared with the values for age-matched WT mice.

cDNA microarray analysis

In order to identify genes whose expression levels were changed in the TG kidney, we carried out cDNA microarray analysis of mouse kidneys at 12 weeks of age. Genes with mean fold change above 2.00 (17 genes including cyclin D2 and osteopontin) or less than 0.60 (12 genes including ornithine decarboxylase) were listed in Table 1.

Immunohistochemical detection of osteopontin and F4/80

Since osteopontin has been reported to induce infiltration of macrophages [10], we performed immunohistochemical detection of osteopontin and macrophage marker F4/80 [11] in the kidneys of TG and WT mice at 20 weeks of age. The glomeruli and the tubular epithelial cells were much more strongly stained for osteopon-

Table 1
Genes up- or down-regulated in CaM kinase IIα (Thr286Asp) transgenic kidney.

Gene name	Function	GenBank No.	Fold
Up-regulated			
Cyclin D2	Cell-cycle	NM_009829	6.70
Sodium channel, nonvoltage-gated 1 beta	Ion transport	NM_011325	4.40
Nectin-lke 1	Calcium ion binding	NM_053199	3.40
Notch-regulated ankyrin repeat protein	Regulation of transcription	NM_025980	3.30
Calcium channel, voltage-dependent, gamma subunit 3	Calcium ion transport	NM_019430	3.21
Pleckstrin homology domain containing, family B member 1	Protein binding	NM_013746	3.18
RAS protein activator like 1	GTPase activator activity	NM_013832	3.12
Receptor-interacting serine-threonine kinase 3	IκB kinase/ NFκB cascade	NM_019955	2.99
Membrane-spanning 4-domains, subfamily A, member 6D	Signal transduction	NM_026835	2.72
Granzyme A	Apoptosis	NM_010370	2.57
Osteopontin	Immune response	NM_009263	2.35
Guanine nucleotide binding protein, alpha 11	G-Protein signaling pathway	NM_010301	2.34
Hydroxyacid oxidase 3	Fatty acid metabolic process	NM_019545	2.23
Lipopolysaccharide binding protein	Lipid binding	NM_008489	2.15
Interleukin 21 receptor	Interleukin receptor activity	NM_021887	2.15
Interleukin enhancer binding factor 3	Protein amino acid methylation	NM_010561	2.06
Catenin delta 2	Cell adhesion	NM_008729	2.00
Down-regulated			
Tumor rejection antigen gp96	Molecular chaperone	NM_011631	0.59
Solute carrier family 21, member 1	Renal organic anion transport	NM_013797	0.58
Carbonic anhydrase 4	Renal bicarbonate reabsorption	NM_007607	0.56
Testis specific gene A2	Sperm mobility	NM_025290	0.55
Pleckstrin	T-cell activation	NM_019549	0.53
Hydroxysteroid 11-beta dehydrogenase 1	Cortisol metabolism	NM_008288	0.51
Lipoprotein lipase	Lipid transporter activity	NM_008509	0.473
Lymphocyte antigen 6 complex, locus E	GPI anchor binding	NM_008529	0.460
Mpv17 transgene, kidney disease mutant-like	Molecular function	NM_033564	0.421
Mouse ornithine decarboxylase	Polyamine biosynthesis	NM_013614	0.348
DNA segment, Chr 7, Roswell Park 2 complex, expressed	Hydrolase activity	NM_033080	0.332
Hemoglobin, beta adult minor chain	Iron ion binding	NM_016956	0.205

The fold changes are mean comparisons between transgenic kidney and wild-type kidney.

tin in the TG kidney (Fig. 3B) as compared to the WT kidney (Fig. 3A). The tubulointerstitium was more strongly stained for F4/80 in the TG kidney (Fig. 3D) as compared to the WT kidney (Fig. 3C).

M1, M2 macrophage-associated mRNA expression

The levels of M1 and M2 macrophage-associated mRNAs in renal cortex of mice were examined by quantitative real-time RT-

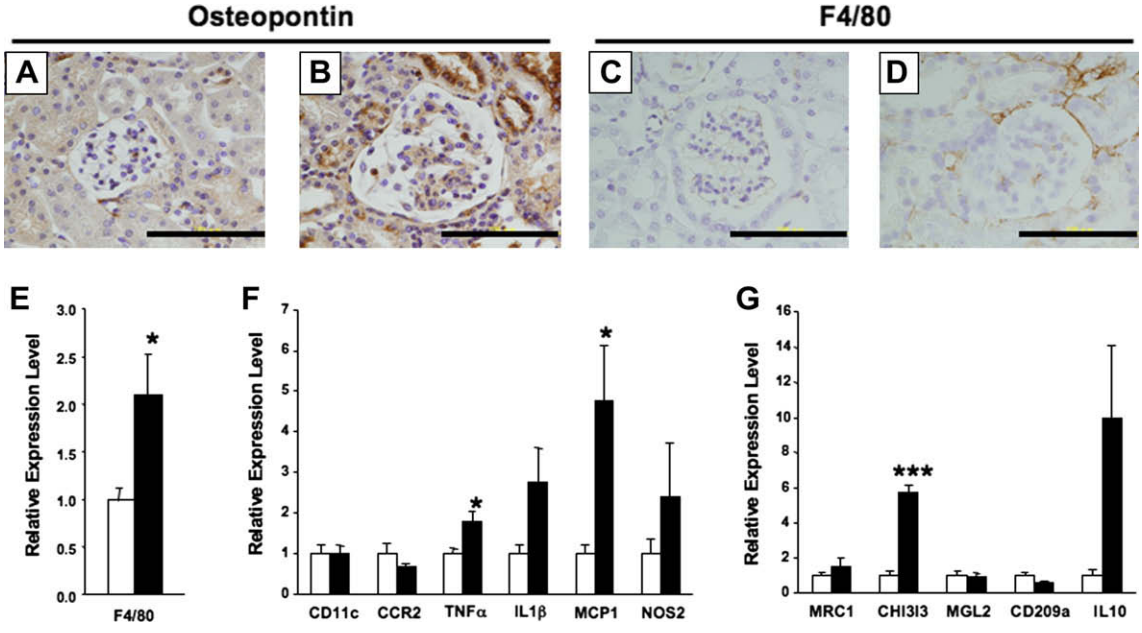

Fig. 3. Immunohistochemical detection of osteopontin (A, B) and F4/80 protein (C, D) in the kidneys of WT mice (A, C) and TG mice (B, D) at the age of 20 weeks. Images are representative from studies of $n = 2$ mice for each genotype. Scale bars = 100 μm. Quantitative real-time PCR analyses of macrophage marker mRNAs in renal cortex at the age of 20 weeks (E–G). (E) mRNA levels of F4/80 as a pan-macrophage marker. (F) mRNA levels of M1 macrophage markers (CD11c, CCR2, TNFα, IL1β, MCP1, and NOS2). (G) mRNA levels of M2 macrophage markers (MRC1, CHI3l3, MGL2, CD209a, and IL10). In (E)–(G), the respective mRNA levels normalized to 18S ribosomal RNA (internal control) levels were shown. White bars and black bars indicate means ± SE for WT mice and TG mice, respectively. Statistical analyses were performed by Student's *t*-test. $^{*}p < 0.05$; $^{***}p < 0.001$ compared with the values for age-matched WT mice.

PCR. The mRNA level of F4/80, a mouse pan-macrophage marker, was significantly higher (2.09-fold, $p < 0.05$) in the TG mice compared to WT mice (Fig. 3E). M1 macrophage markers such as CD11c, chemokine CCmotif receptor 2 (CCR2), tumor necrosis factor α (TNFα), interleukin-1β (IL-1β), monocyte chemotactic protein-1 (MCP-1), and nitric oxide synthase 2 (NOS2) were then analyzed. Among them, the mRNA levels of TNFα (1.77-fold) and MCP-1 (4.77-fold) were significantly higher ($p < 0.05$ for both) in the TG mice compared to WT mice (Fig. 3F). M2 macrophage markers such as mannose receptor C-type1 (MRC1), chitinase 3-like 3 (CHI3l3), macrophage galactose N-acetyl-galactosamine specific lectin 2 (MGL2), CD209a, and interleukin-10 (IL-10) were next analyzed. Among them, the mRNA level of CHI3l3 (5.72-fold) was significantly higher ($p < 0.001$) in the TG mice compared to WT mice (Fig. 3G).

Discussion

Recently we generated TG mice overexpressing the mutant form (Thr286Asp) of CaM kinase IIα in pancreatic β-cells and reported that they serve as a novel model of severe insulin-dependent diabetes [7]. In the present study, the TG mice maintained high levels of blood glucose and hemoglobin A_{1c}. Urinary albumin/creatinine ratio as well as serum BUN level were significantly elevated in the TG mice (Fig. 1), indicating that TG renal function is impaired. Histological analyses of kidneys revealed that glomerular area, mesangial area, and mesangial/glomerular area ratio all increased in the TG mice (Fig. 2).

Renal hypertrophy is known as one of the pathological characters in early diabetic nephropathy. The activation of cyclin D kinase activity is thought to play important roles in the growth of kidney, especially by inducing renal tubule epithelial cell hypertrophy in a cell cycle-dependent fashion [12]. Interestingly, the up-regulated expression of cyclin D2 mRNA (6.70-fold) was found in the TG kidney by cDNA microarray analysis (Table 1). Since cyclin D2 activates cyclin D kinase and by doing so, promotes the progression of cell cycle, it should be reasonable to assume that cyclin D2 plays an important role in the process of renal hypertrophy in the TG mice.

Osteopontin is a chemokine-like, extracellular matrix-associated protein with diverse functions [10,13]. In the present study, the expression of osteopontin was increased by 2.35-fold in the TG kidney (Table 1). The elevated expression of osteopontin in renal cortex has also been reported in murine models of diabetes such as streptozotocin-induced diabetic rats [14] and *db/db* mice [15]. Osteopontin is now supposed to play important roles in the formation of renal lesions in DM. However, little was known how osteopontin contributes to the progression of diabetic nephropathy.

One of the osteopontin's functions is to locally recruit monocytes and induce inflammatory immune response [13]. Macrophage infiltration has been reported to increase in diabetic kidneys and thought to play significant roles in the progression of diabetic nephropathy [16,17]. However, the characters of macrophages infiltrated in diabetic kidneys were not well documented. There are at least two subtypes of resident macrophages in tissues [18]. One is referred to as M1 macrophages, that are classically activated by Th1 stimuli. M1 macrophages express high levels of proinflammatory cytokines and enhances tissue inflammatory response. Another is M2 macrophages, that are alternatively activated by Th2 stimuli. M2 macrophages express high levels of anti-inflammatory cytokines such as IL-10, and participate in the promotion of tissue repair, remodeling and vasculogenesis. To determine which types of macrophages are dominant in the TG kidneys, we performed real-time RT-PCR analyses for various macrophage marker RNAs (Fig. 3). M1 macrophage markers such as TNFα and MCP1, as well as M2 macrophage marker such as CHI3l3 were elevated in renal cortex of TG mice. This result indicates that not only M1 macrophages but also M2 macrophages participate in the formation of diabetic nephropathy in the TG mice.

Overall results indicate that the CaM kinase IIα (Thr286Asp) TG mice can serve as an excellent model for diabetic nephropathy. We are now challenging to identify expression patterns of the individual genes up-regulated and down-regulated in the TG kidney (Table 1; total 29 genes) both at the RNA level and at the protein level. By doing so, it should be eventually possible to identify genes responsible for diabetic nephropathy and develop potential therapies against it.

Acknowledgments

We thank Takako Matsushima, Tomomi Kubo, and Sayaka Kobayashi for technical assistance.

References

[1] R.P. Robertson, Chronic oxidative stress as a central mechanism for glucose toxicity in pancreatic islet beta cells in diabetes, J. Biol. Chem. 279 (2004) 42351–42354.
[2] M. Brownlee, A radical explanation for glucose-induced beta cell dysfunction, J. Clin. Invest. 112 (2003) 1788–1790.
[3] M. Krolewski, P.W. Eggers, J.H. Warram, Magnitude of end-stage renal disease in IDDM: a 35 year follow-up study, Kidney Int. 50 (1996) 2041–2046.
[4] J.M. Steinke, M. Mauer, Lessons learned from studies of the natural history of diabetic nephropathy in young type 1 diabetic patients, Pediatr. Endocrinol. Rev. 5 (Suppl 4) (2008) 958–963.
[5] T. Doi, M. Hattori, L.Y. Agodoa, T. Sato, H. Yoshida, L.J. Striker, G.E. Striker, Glomerular lesions in nonobese diabetic mouse: before and after the onset of hyperglycemia, Lab. Invest. 63 (1990) 204–212.
[6] J.R. Williamson, K. Chang, R.G. Tilton, C. Prater, J.R. Jeffrey, C. Weigel, W.R. Sherman, D.M. Eades, C. Kilo, Increased vascular permeability in spontaneously diabetic BB/W rats and in rats with mild versus severe streptozocin-induced diabetes. Prevention by aldose reductase inhibitors and castration, Diabetes 36 (1987) 813–821.
[7] I. Kato, T. Oya, H. Suzuki, K. Takasawa, A.M. Ichsan, S. Nakada, Y. Ishii, Y. Shimada, M. Sasahara, K. Tobe, S. Takasawa, H. Okamoto, K. Hiraga, A novel model of insulin-dependent diabetes with renal and retinal lesions by transgenic expression of CaMKIIalpha (Thr286Asp) in pancreatic beta-cells, Diabetes Metab. Res. Rev. 24 (2008) 486–497.
[8] I. Shimada, K. Matsui, B. Brinkmann, C. Hohoff, K. Hiraga, Y. Tabuchi, I. Takasaki, I. Kato, H. Kawaguchi, K. Takasawa, R. Iida, H. Takizawa, T. Matsuki, Novel transcript profiling of diffuse alveolar damage induced by hyperoxia exposure in mice normalization by glyceraldehyde 3-phosphate dehydrogenase, Int. J. Legal Med. 122 (2008) 373–383.
[9] K.O. Alsaad, A.M. Herzenberg, Distinguishing diabetic nephropathy from other causes of glomerulosclerosis: an update, J. Clin. Pathol. 60 (2007) 18–26.
[10] M. Scatena, L. Liaw, C.M. Giachelli, Osteopontin: a multifunctional molecule regulating chronic inflammation and vascular disease, Arterioscler. Thromb. Vasc. Biol. 27 (2007) 2302–2309.
[11] J.M. Austyn, S. Gordon, F4/80, a monoclonal antibody directed specifically against the mouse macrophage, Eur. J. Immunol. 11 (1981) 805–815.
[12] P. Preisig, A cell cycle-dependent mechanism of renal tubule epithelial cell hypertrophy, Kidney Int. 56 (1999) 1193–1198.
[13] D.T. Denhardt, X. Guo, Osteopontin: a protein with diverse functions, FASEB J. 7 (1993) 1475–1482.
[14] J.W. Fischer, C. Tschöpe, A. Reinecke, C.M. Giachelli, T. Unger, Upregulation of osteopontin expression in renal cortex of streptozotocin-induced diabetic rats is mediated by bradykinin, Diabetes 47 (1998) 1512–1518.
[15] K. Susztak, E. Böttinger, A. Novetsky, D. Liang, Y. Zhu, E. Ciccone, D. Wu, S. Dunn, P. McCue, K. Sharma, Molecular profiling of diabetic mouse kidney reveals novel genes linked to glomerular disease, Diabetes 53 (2004) 784–794.
[16] F. Chow, E. Ozols, D.J. Nikolic-Paterson, R.C. Atkins, G.H. Tesch, Macrophages in mouse type 2 diabetic nephropathy: correlation with diabetic state and progressive renal injury, Kidney Int. 65 (2004) 116–128.
[17] F.Y. Chow, D.J. Nikolic-Paterson, R.C. Atkins, G.H. Tesch, Macrophages in streptozotocin-induced diabetic nephropathy: potential role in renal fibrosis, Nephrol. Dial. Transplant. 19 (2004) 2987–2996.
[18] S. Gordon, Alternative activation of macrophages, Nat. Rev. Immunol. 3 (2003) 23–35.